ENVIRONMENTAL RESEARCH LETTERS

PURPOSE-LED PUBLISHING™ Part of the ENVIRONMENTAL RESEARCH SERIES

LETTER • OPEN ACCESS

Effects of extreme stratospheric polar vortex events on near-surface wind gusts across Europe

To cite this article: Eduardo Utrabo-Carazo *et al* 2024 *Environ. Res. Lett.* **19** 094044

ENVIRONMENTAL RESEARCH
LETTERS

RECEIVED
20 May 2024

REVISED
15 July 2024

ACCEPTED FOR PUBLICATION
26 July 2024

PUBLISHED
19 August 2024

LETTER

Effects of extreme stratospheric polar vortex events on near-surface wind gusts across Europe

Eduardo Utrabo-Carazo[1,*], **Julia F Lockwood**[2], **Robert J H Dunn**[2], **Lorenzo Minola**[1,3,4], **Enric Aguilar**[5] and **Cesar Azorin-Molina**[1]

[1] Centro de Investigaciones sobre Desertificación, Consejo Superior de Investigaciones Científicas (CIDE, CSIC-UV-Generalitat Valenciana), Climate, Atmosphere and Ocean Laboratory (Climatoc-Lab), Moncada, Valencia, Spain
[2] Met Office Hadley Centre, Exeter, United Kingdom
[3] Regional Climate Group, Department of Earth Sciences, University of Gothenburg, Gothenburg, Sweden
[4] Interuniversity Department of Regional and Urban Studies and Planning (DIST), Politecnico and University of Turin, Turin, Italy
[5] Centre for Climate Change, Universitat Rovira i Virgili, Tarragona, Spain
[*] Author to whom any correspondence should be addressed.

E-mail: eduardo.utrabo@ext.uv.es

Keywords: wind gusts, polar vortex, extreme events, sudden stratospheric warmings

Supplementary material for this article is available online

Abstract

Extreme stratospheric polar vortex (SPV) events can influence winter tropospheric circulation for up to 60 d. Their impacts on air temperature have been extensively studied recently. However, there is a research gap in their effects on wind speeds and its extremes. This study aims to evaluate, for the first time, the impacts of such extreme SPV events on observed and modelled near-surface wind gusts across Europe. We have analysed wind gust data coming from: station-based observations (for the Iberian Peninsula and Scandinavia), the ERA5 reanalysis and the SEAS5 and GloSea6 seasonal forecasting systems. We assess their similarities in reproducing 4 parameters of their corresponding distributions: median, standard deviation, skewness and kurtosis. For all these datasets, the results indicate that extreme positive SPV events are followed by negative wind gust anomalies in Southern Europe and positive in Northern Europe. Whereas, negative SPV events (such as Sudden Stratospheric Warmings) have positive gust anomalies in Southern Europe and negative in the north. A central region shows negligible anomalies in both cases. This highlights the ability of SPV as a predictor for short-medium-term forecasting of extreme wind events, which would have direct applications to many socioeconomic and environmental issues such as the estimation of wind-power generation.

1. Introduction

The stratospheric polar vortex (SPV) is a region of strong westerly circumpolar winds that forms between November and March in the Northern Hemisphere due to the temperature gradient between the mid-latitudes and the North Pole (Waugh *et al* 2017). Stratospheric Sudden Warmings (SSW) correspond to the negative extremes in the SPV. They occur when the SPV shifts from its usual location or weakens until it breaks, increasing the polar stratosphere temperature by tens of degrees (Baldwin *et al* 2021). Both positive (strong westerly flow) and negative (easterly flow) extreme SPV can influence the troposphere for months (Smith *et al* 2018). These phenomena have received significant attention recently because of their potential as surface weather predictors (Büeler *et al* 2020) on a wide range of scales: monthly, seasonal, etc (Kidston *et al* 2015). Their effects on air temperature have been extensively studied (e.g. King *et al* 2019), along with the changes in weather regimes they produce (Ayarzagüena *et al* 2018). However, there is a research gap on their influence on near-surface mean wind speed and gusts, despite their impacts on the environment and society (e.g. Tian *et al* 2019).

Not all extreme SPV events influence the troposphere. It is still unclear which tropospheric precursors determine their surface impacts (e.g. Bett *et al* 2023). The canonical response after an SSW with tropospheric signal is a negative North Atlantic Oscillation (NAO) phase (Baldwin *et al* 2021). Nevertheless, Beerli and Grams (2019) demonstrated SSW can be also associated with atmospheric circulation patterns different from a negative NAO depending on the previous tropospheric conditions. Similarly, Minola *et al* (2016) and Utrabo-Carazo *et al* (2022) showed that, although high, the correlations between the NAO and near-surface wind speed in winter do not exceed 0.70 for the Iberian Peninsula (IP) and Scandinavia, respectively. Therefore, near-surface wind speed changes in these regions are affected by other atmospheric circulation patterns in addition to the NAO during winter. Relatively few extreme SPV events have occurred in the observational period, limiting the understanding of their impacts in the troposphere (Kolstad *et al* 2022). Scherhag (1952) was a pioneer in observing an SSW from radiosondes in early 1952, and about 35 SSWs were then observed for ∼1950–2022 (Hall *et al* 2021). Consequently, climate models are crucial to increase the pool of such events. Bett *et al* (2023) demonstrated the ability of seasonal prediction systems (SPS) to reproduce the SSW frequency and impacts on the troposphere, while Lockwood *et al* (2023) demonstrated their ability to predict winds and storms, especially in winter.

Changes in mean sea level pressure (MSLP) following an extreme SPV event should have a large influence on near-surface wind speed (Baldwin *et al* 2021). White *et al* (2020) revealed that after an SSW the jet stream moves equatorward, and vice versa for extreme positive SPV. Furthermore, Utrabo-Carazo *et al* (2023) revealed a close relationship between the SPV and observed near-surface wind speed over the IP, with a time lag of approximately 2 months. They found a negative correlation between SPV and near-surface wind speed, but nothing was discussed about their magnitude or spatial distribution. Therefore, extreme SPV events could be a reliable prediction source for both mean and extreme wind speed (Domeisen and Butler 2020). As it is still unclear the impact of extreme SPV events (especially when it comes to positive extremes) on wind gusts, this study aims to quantify for the first time their effects on daily peak wind gusts (DPWG) focusing on the IP and Scandinavia. Specifically, our research questions are:

1. How do observed DPWG change after an extreme SPV event?
2. Are there significant differences in DPWG between extreme negative (SSW) and positive SPV events?
3. Can the ERA5 reanalysis, and SEAS5 and GloSea6 SPS reproduce the observed DPWG under extreme SPV events?

2. Data and methods

2.1. Observed and model data

We used two observational DPWG datasets covering Southern Europe (87 stations across Spain and Portugal, i.e. IP; 1961–2019) and Northern Europe (127 stations across Finland, Norway and Sweden, i.e. Scandinavia; 1996–2016), where the correlation of the NAO index with DPWG has an opposite sign: negative for the IP (Utrabo-Carazo *et al* 2022) and positive for Scandinavia (Minola *et al* 2016, 2023). The DPWG is defined as the 10 m height maximum wind speed recorded as a 3 s (2 s for Sweden) mean over 24 h. Both datasets have been quality controlled and homogenized through the R package Climatol (available online at https://CRAN.R-project.org/package=climatol; last accessed 14 May 2024) and details can be found in Minola *et al* (2021) and Utrabo-Carazo *et al* (2022).

Due to the scarcity in the availability of DPWG observations across Europe, we also used reanalysis and SPS outputs. We chose the ECMWF Reanalysis v5 (ERA5; Hersbach *et al* 2023) as it has been shown to currently be the best reanalysis in representing observed near-surface wind speed (Ramon *et al* 2019). We covered 72 winters from 1950–1951 to 2021/2022. To create the DPWG series from ERA5, it is selected the maximum value of the 24 available for each day of the variable '10 m wind gust since previous post-processing' across the 10° W–40° E and 35° N–72° N domain at 0.25° × 0.25°. For the NAO definition, MSLP outputs are downloaded, while for the SPV definition, we accessed the zonal-mean zonal wind at the 10 hPa level and 60° N.

For robustness of the results and comparison purposes with the work of Bett *et al* (2023) for GloSea5, the hindcast data from two SPS datasets were chosen: (i) the ECMWF SPS (SEAS5; Johnson *et al* 2019), and (ii) the Met Office Global Seasonal Forecasting System version 6 (GloSea6; MacLachlan *et al* 2015). For those datasets, the same variables and domains used for ERA5 are chosen. For SEAS5 (available at 1° × 1°), they are accessed 25 members of version 51 for 1981–2016, all initialised on November 1st, therefore, 25 × 1 × 36 × 1 = 900 winters. For GloSea6 (available at 1° x 1°) 7 members of versions 601 and 602 are accessed for 1993–2016, initialised on 25 October, 1st November and 9 November, therefore, 7 × 2 × 24 × 3 = 1008 winters. Three initial dates are selected to have a comparable number of winters between SEAS5 and GloSea6.

2.2. Methods

We compute the DPWG anomalies for the observations, ERA5 and the two SPS; and the daily MSLP anomalies for ERA5 and the two SPS. Anomalies are calculated as deviations from the mean of the whole period available for each product. Such mean is smoothed by a Gaussian filter with a 10 d window to reduce the high-frequency variability following Bett *et al* (2023). The NAO index is calculated as the difference between the MSLP anomalies of a box region around Iceland (25°–16° W, 63°–70° N) and the Azores (28°–20° W, 36°–40° N), following Dunstone *et al* (2016).

We distinguish two types of extreme SPV during the boreal winter (i.e. December–January–February): (a) SSW events, i.e. when the 60° N zonal-mean zonal wind speed at 10 hPa drops below 0 m s^{-1} (∼5th of the SPV series in ERA5; Baldwin *et al* (2021); and (b) Strong Stratospheric Polar Vortex (SSPV) events, i.e. when that same variable exceeds 55 m s^{-1} (∼95th of the SPV series in ERA5). Due to the lack of commonly accepted criteria in the SSPV definition, the 55 m s^{-1} value has been chosen for consistency with the classical SSW definition (5th percentile *vs.* 95th percentile) and to have a close number of events of each type in ERA5 (35 SSW *vs.* 34 SSPV). As for Bett *et al* (2023), we defined that each of these extreme SPV events has a signal in the troposphere if the mean NAO index in the 30 d following the event is negative for SSWs or positive for SSPVs.

To demonstrate that ERA5 and both SPS reproduce the observed DPWG anomalies over the IP and Scandinavia, 4 parameters (median, standard deviation, skewness and kurtosis) are compared. We compare the DPWG anomaly distributions and not the actual DPWG distributions as we expect a bias between the observed and modelled gusts and we are interested in the change produced by the extreme SPV events, not the magnitude of the gusts themselves. Additionally, to check that the SPS correctly simulate the extreme SPV events and their effects in the troposphere, 3 parameters are compared with those for ERA5: (a) the fraction of winters with at least one SSW or SSPV; (b) the proportion of such events with a tropospheric signal; and (c) the magnitude of that signal in the NAO for each extreme SPV event and the mean NAO for all SSWs and all SSPVs. We perform a resampling by making 1000 pseudoseries of 72 winters by taking years and members randomly from the ensemble. We do this to compare fairly between ERA5 and the SPS, with each element having the same winters as those available in ERA5. We use the Wilson score interval (Wilson 1927) to determine the confidence intervals and a binomial test to determine their difference from a given value (e.g. Brown *et al* 2001). These tests are performed at the 5% significance level following Bett *et al* 2023. In addition, we calculate 5000 random 30 d periods of the NAO in DJF to test the prevalence of negative values of this index in the SPS.

We calculate the DPWG anomaly mean in the 30 d following each extreme SPV event and make two groups on which we will average: (i) all events with a tropospheric signal, and (ii) all the events regardless of whether they have a tropospheric signal or not. We define those two groups because the current state-of-the-art does not allow us to distinguish between them *a priori* in the short-term prediction (Baldwin *et al* 2021). Finally, we determine the differences in DPWG anomalies between the results for SSW and SSPV events and the statistical significance of the differences by a Student's t-test at a 1% significance level. The results have been repeated for 1–60 d after each episode to check the signal persistence in the troposphere.

3. Results

3.1. Validation of model data

A comparison of the DPWG anomaly histograms shows that, except for small deviations, the histograms from the models overlap with the observed ones for the IP and Scandinavia (figure S1 in the Supporting Information). The median is negative in all cases and both observations and ERA5 fall within the distribution of the SPS from the resampling (figures 1 and 2 for SEAS5 and figures S2 and S3 for GloSea6). The median for the IP is more negative than for Scandinavia. All distributions have positive skewness, as expected since DPWG has a lower limit at 0 m s^{-1}. The observation skewness is within the SPS resampling distribution, while ERA5 skewness is in the left tail. All distributions are leptokurtic, being the kurtosis coefficient slightly higher for the SPS than for the observations and ERA5. Overall, there is a good agreement in all parameters (except for the standard deviation) between observed and modelled datasets for both regions. The differences are small relative to their absolute values, with the largest mismatches found in the standard deviations. These results give us confidence in the extrapolation of the results across Europe for 1950–2022 (see section 4).

Figure 3 compares how ERA5 and SEAS5 (GloSea6 in figure S4) simulate the SSW occurrence and their effects on the troposphere, specifically on the NAO. Figure 4 (figure S5 for GloSea6) represents the same but for SSPVs. Table 1 shows these results in percentages with their confidence intervals. Both SPS overestimate and underestimate the proportion of SSWs and SSPVs per winter, respectively. However, they simulate almost perfectly the proportion of events that have a signal in the NAO, negative for SSWs and positive for SSPVs; with GloSea6 performing particularly well in this respect. Nevertheless, the magnitude of this signal is slightly overestimated, in absolute value, for both SSW and SSPV, although the ERA5 values fall within the distribution coming from both system's resampling.

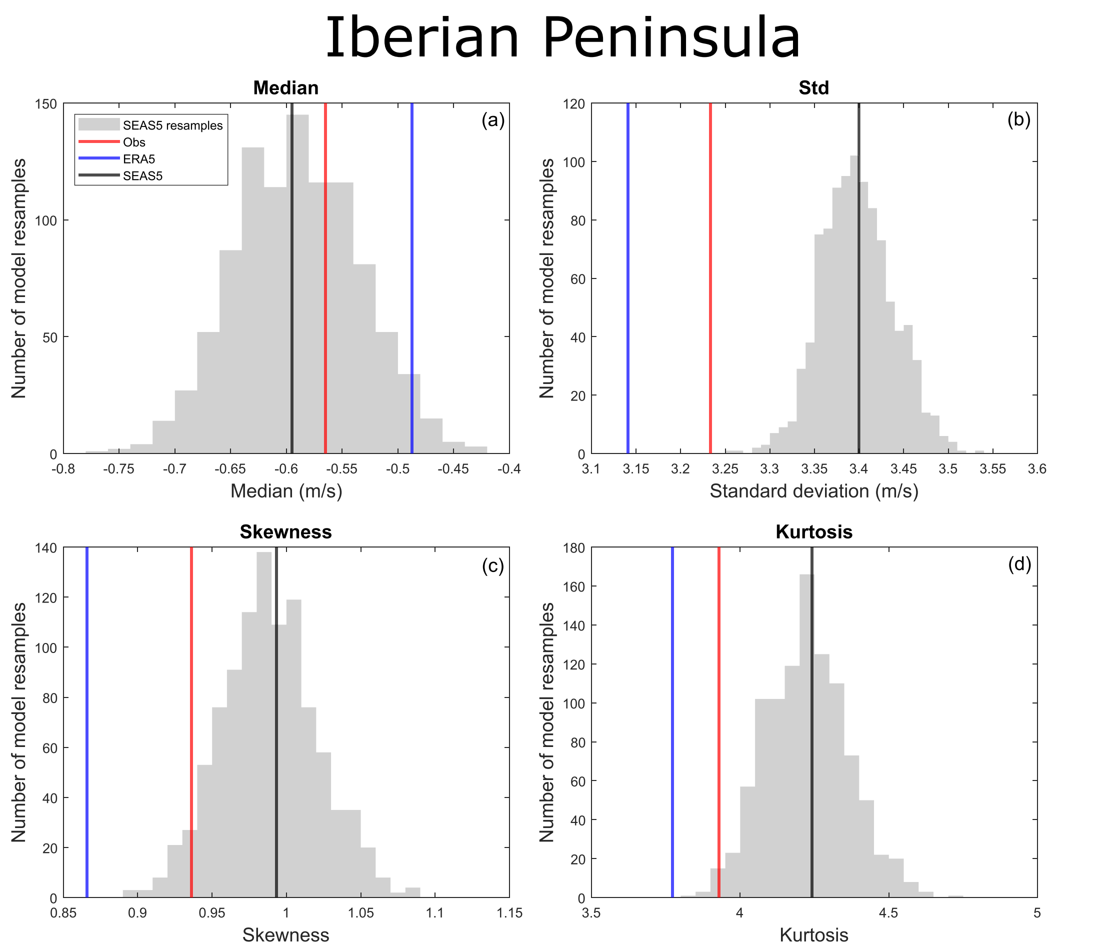

Figure 1. Comparative analysis of DPWG anomalies distributions over the IP from observations (red), ERA5 reanalysis (blue), SEAS5 seasonal forecasting system (black) and model resampling (grey) for: (a) median, (b) standard deviation, (c) skewness and (d) kurtosis. The distributions of the SEAS5 parameters are taken from the 1000 bootstrapped samples.

3.2. Impact of extreme SPV events on DPWG anomalies from observations

For the IP, we find positive DPWG anomalies after SSW and negative anomalies after SSPV, except for the mouth of the Ebro in north-eastern IP for SSPV where they are slightly positive (figure 5). These results are analogous for both 1–30 and 1–60 d later (figure S6), as well as when considering all events or only those with tropospheric signal. The largest differences between DPWG anomalies after an SSW and after an SSPV occur in the IP western half when considering only events with a tropospheric signal. This west-east pattern disappears when considering all events together. Such differences reach 2 m s^{-1} in more than 10% of the stations. For Scandinavia (figure 6), the pattern is reversed, consistent with the expectation of a negative NAO phase following an SSW, and a positive NAO phase following an SSPV. Widespread negative DPWG anomalies appear after SSW and positive anomalies after SSPV. The largest differences occur in the western half of Scandinavia. Such differences reduce when looking at 1–60 d after (figure S7) and considering all events regardless of the tropospheric signal. It is remarkable the appearance of negative anomalies after an SSPV considering all events in northern Norway between 1–60 d

Note that: (a) none of the differences in any case and for any station is statistically significant ($p > 0.01$) for either the IP or Scandinavia given the small number of events available in the observation period; and (b) the absolute magnitudes of the DPWG anomalies are higher for Scandinavia than for the IP, probably due to the shorter period available (1996–2016 vs. 1961–2019), so fewer SSWs and SSPV events and thus the signal is less diluted by averaging over fewer events.

3.3. Impact of extreme SPV events on DPWG anomalies from ERA5 reanalysis

The DPWG anomalies after extreme SPV events for ERA5 across Europe (figure 7) show the same North–South pattern as for the observations. It is possible now to identify a transition region in central Europe where the anomalies are zero, this zone was not sampled by the observations. This transition region is slightly further north for the SSPVs than for the SSWs. In southern Europe, the anomalies are roughly uniform in magnitude, while for northern

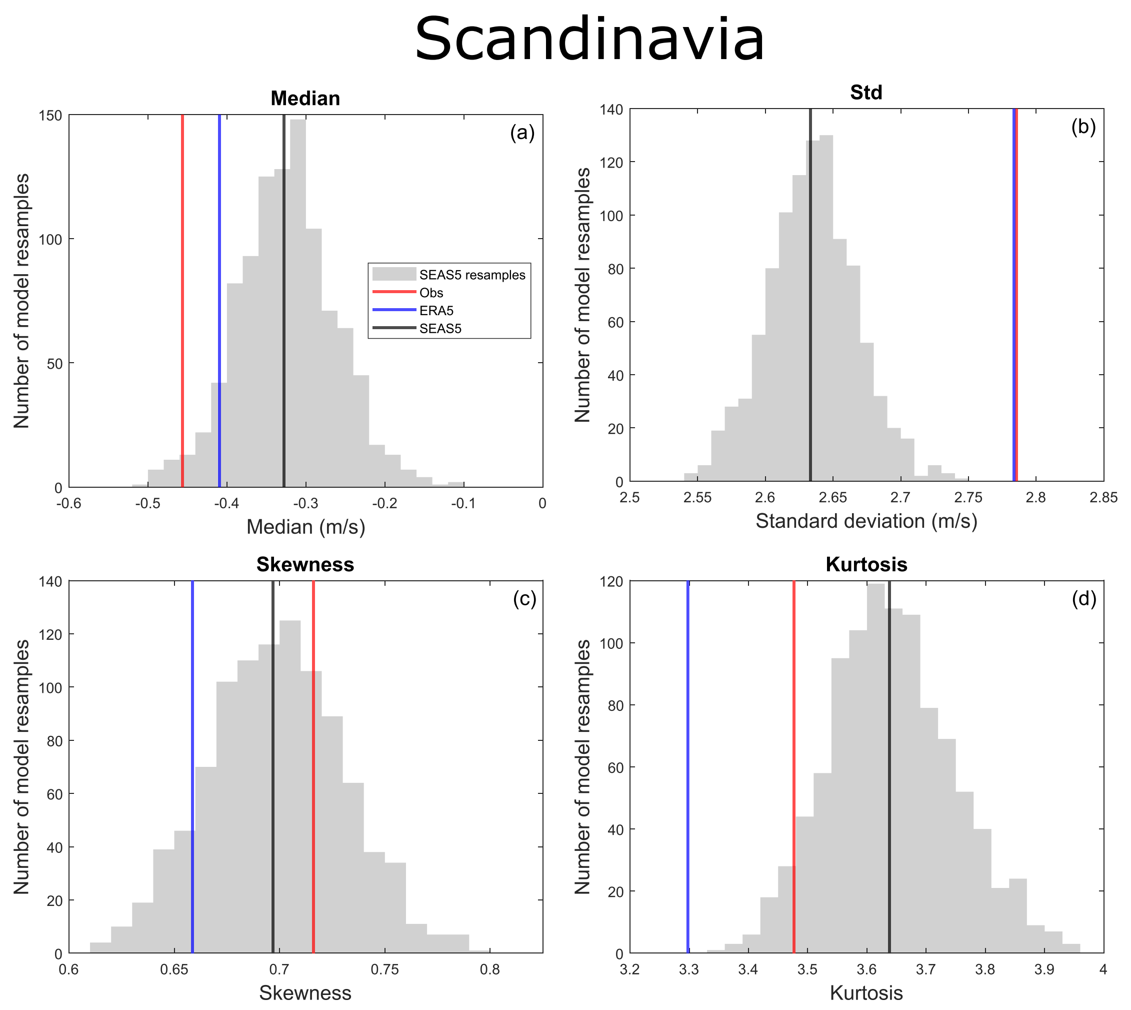

Figure 2. As in figure 1 but for Scandinavia.

Europe, the most negative (positive) anomalies for SSW (SSPV) occur across the North Sea upper half, especially over north of the British Isles and over the westernmost coasts of Norway near Bergen.

The differences between SSW minus SSPV are statistically significant at all locations when considering only the events with tropospheric signal, and only in northern and southern Europe when considering all the events. This is repeated for both 1–30 d and 1–60 d (figure S8). Generally, the anomalies decrease in magnitude when comparing between 1–30 and 1–60 and between events with tropospheric signal and all the events.

3.4. Impact of extreme SPV events on DPWG anomalies from SPSs

Figure 8 shows DPWG anomalies after extreme SVP events as simulated by SEAS5 (figure S9 for GloSea6), the simulated patterns are practically analogous to the ones modelled by ERA5, considering the lower SPS spatial resolution. In this case, we do not detect the northward shift in the transition region for the SSPVs that we saw in the results from ERA5. The uniformity in the anomalies in southern Europe and the centers of greatest anomalies on the southern coasts of the British Isles and the coasts around Bergen (Norway) are maintained. The statistical significance is also repeated in the differences compared to ERA5, all differences are statistically significant when considering only the events with tropospheric signal and only the northern and southern regions are statistically significant when considering all events, this is repeated for 1–60 d later for both SEAS5 (figure S10) and GloSea6 (figure S11). Again, the anomalies are larger in magnitude between 1–30 d than between 1–60 and for only the events with tropospheric signal than for all events.

If we compare GloSea6 and SEAS5 we see larger negative anomalies in northern Europe for GloSea6 after an SSW and larger negative anomalies in southern Europe for SEAS5 after an SSPV. The difference maps are about the same in northern Europe and slightly higher for southern Europe in SEAS5. Finally, the results are analogous between SEAS5 and GloSea6 when considering DPWG anomalies between 1 and 60 d after extreme SPV events.

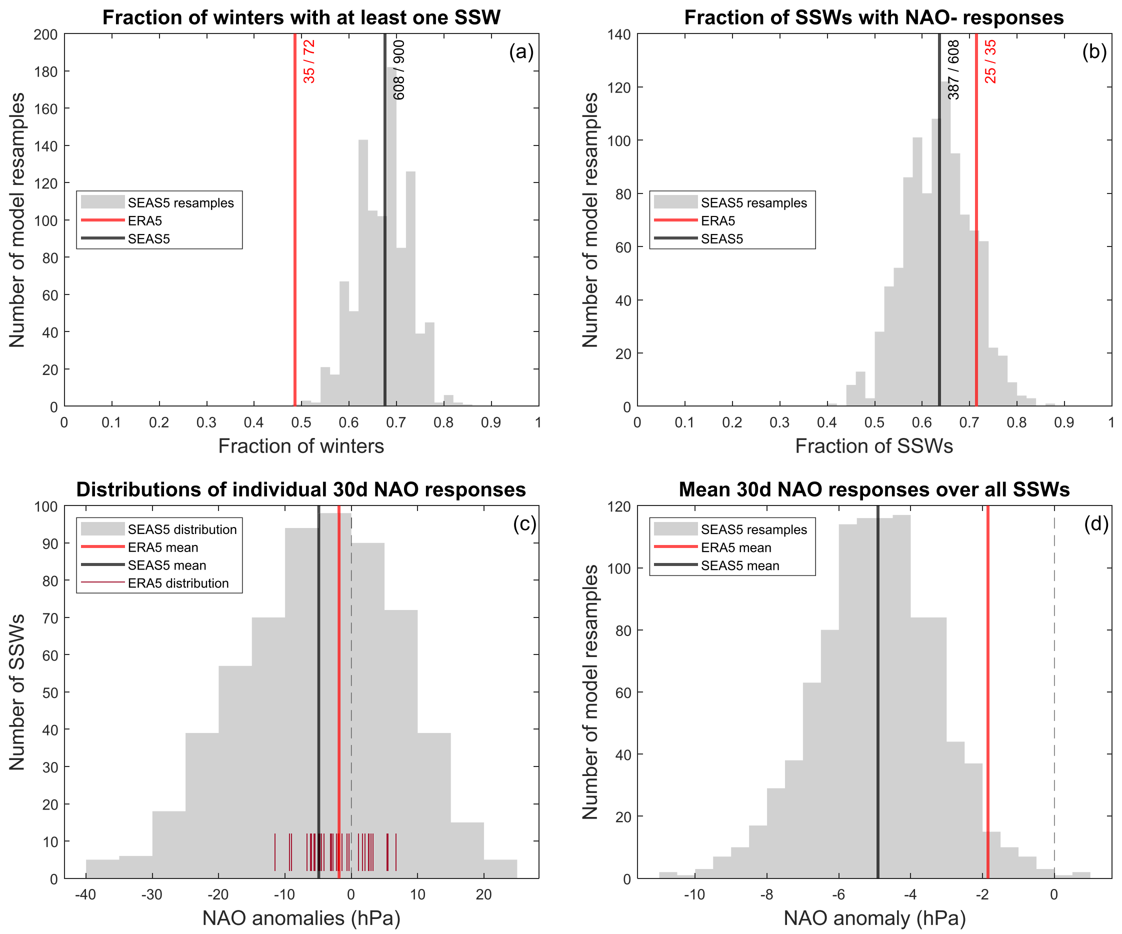

Figure 3. The frequency of SSWs and their NAO responses for ERA5 and SEAS5. Panels show (a) the fraction of winters with at least one SSW in DJF; (b) the fraction of those SSWs with negative NAO responses, based on the mean NAO anomaly in the 30 d following the SSW; (c) the distribution of all post-SSW NAO anomalies; and (d) the mean of those post-SSW anomalies, over all SSWs. All panels use the same colouring: solid vertical lines show the single values from the observations (black) and the model (red), and grey histograms show the distributions of such values over the one thousand 72 year model resamples. In panel (c) the red histogram shows the distribution over the 608 SSWs in the model, and the black ticks at the bottom of the plot show the corresponding observed distribution. Note that the solid vertical lines in panels (c) and (d) show the same means, and the faint dotted vertical lines indicate zero.

Finally, if we consider the opposite NAO indices after the extreme SPV events, i.e. positive NAO after SSW and negative one after SSPV, we see opposite patterns in the DPWG anomalies of much smaller magnitude for the observations, ERA5 and both SPS (figures S12–S16).

4. Discussion

In this study, extreme SPV effects on observed and simulated DPWG are evaluated. Furthermore, the ability of reanalysis and currently available SPSs to reproduce the observed patterns is assessed. As King *et al* (2019) already showed for precipitation and air temperature over Europe, the SPV affects not only the average climate conditions but also its extremes. In general, reliable *in-situ* near-surface wind speed observations, especially DPWG measurements are scarce, cover short periods or are of low quality (Zhou *et al* 2022). Nevertheless, since reanalyses and models in most cases do not accurately reproduce these variables, station-based wind series become crucial. Before using any model product for any wind study, their ability to represent observed wind statistics must be proven by accessing station-based and quality-controlled wind measurements (Ramon *et al* 2019).

We verified how both ERA5 reanalysis and the SEAS5 and GloSea6 SPS reproduce the frequency distribution of observed DPWG anomalies over South (i.e. across the IP) and North (i.e. across Scandinavia) Europe. In both regions, DPWG are highly, and oppositely, correlated in winter with the NAO which is a large-scale pattern. Therefore, it is likely our extrapolation to the rest of Europe is reliable, although it must be tested with DPWG data from other regions. The validity of the temporal extrapolation has not been tested. Models may not capture observed trends, but this is not particularly relevant since we are interested in individual events of relatively short

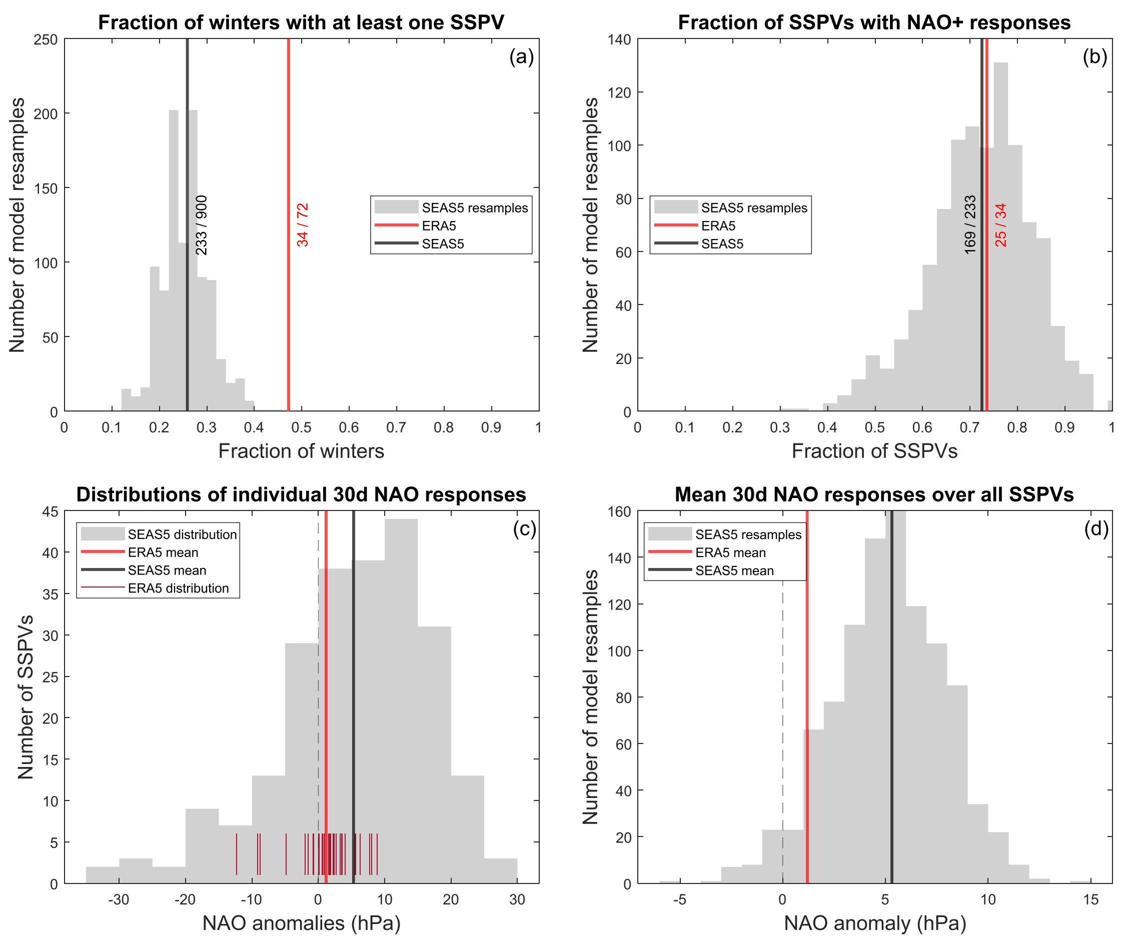

Figure 4. As in figure 3 but for SSPV events and NAO+ in (b).

Table 1. Comparison of the proportion of winters with at least one SSW or SSPV and their corresponding proportions of NAO signals in the ERA5 reanalysis and the SEAS5 and GloSea6 seasonal forecasting systems. The last row shows the probability of finding negative 30 d means in the NAO in random 30 d periods during DJF, for the whole series in ERA5 and in a resample of 5000 winters for SEAS5 and GloSea6. Statistically significant different from 50% at $p < 0.05$ are shown in boldface.

		ERA5	SEAS5	GloSea6
Winters with SSW	Proportion	49%	**68%**	**63%**
	Confidence interval	37%–60%	64%–71%	60%–66%
SSW with negative NAO	Proportion	**71%**	**64%**	**70%**
	Confidence interval	55%–84%	60%–67%	66%–74%
Winters with SSPV	Proportion	47%	**26%**	**29%**
	Confidence interval	36%–59%	23%–29%	26%–32%
SSPV with positive NAO	Proportion	**74%**	**73%**	**74%**
	Confidence interval	57%–85%	67%–78%	69%–79%
30 negative NAO period	Proportion	**46%**	**48%**	**45%**
	Confidence interval	44%–47%	47%–49%	44%–47%

duration and evenly spaced in time. SEAS5 and GloSea6 ability to reproduce near-surface wind speed has been validated in other European regions, both for wind droughts (Kay *et al* 2023) and wind extremes (Owen *et al* 2021). However, they focused on the comparison of ERA5 with SPS, so a novelty of our study relies on using station-based DPWG observations. A possible inconsistency source between observations and models is the DPWG definition, as the models are limited due to parameterization, they could not correctly reproduce observations for certain situations (Minola *et al* 2020).

Bett *et al* (2023) showed the SPS ability to simulate the SSW ratio and its effects in the troposphere compared to ERA5. We also proved they can realistically simulate the SSPV occurrence and their impacts. The effect on the NAO in the 30 d following the extreme SPV event could be considered a first

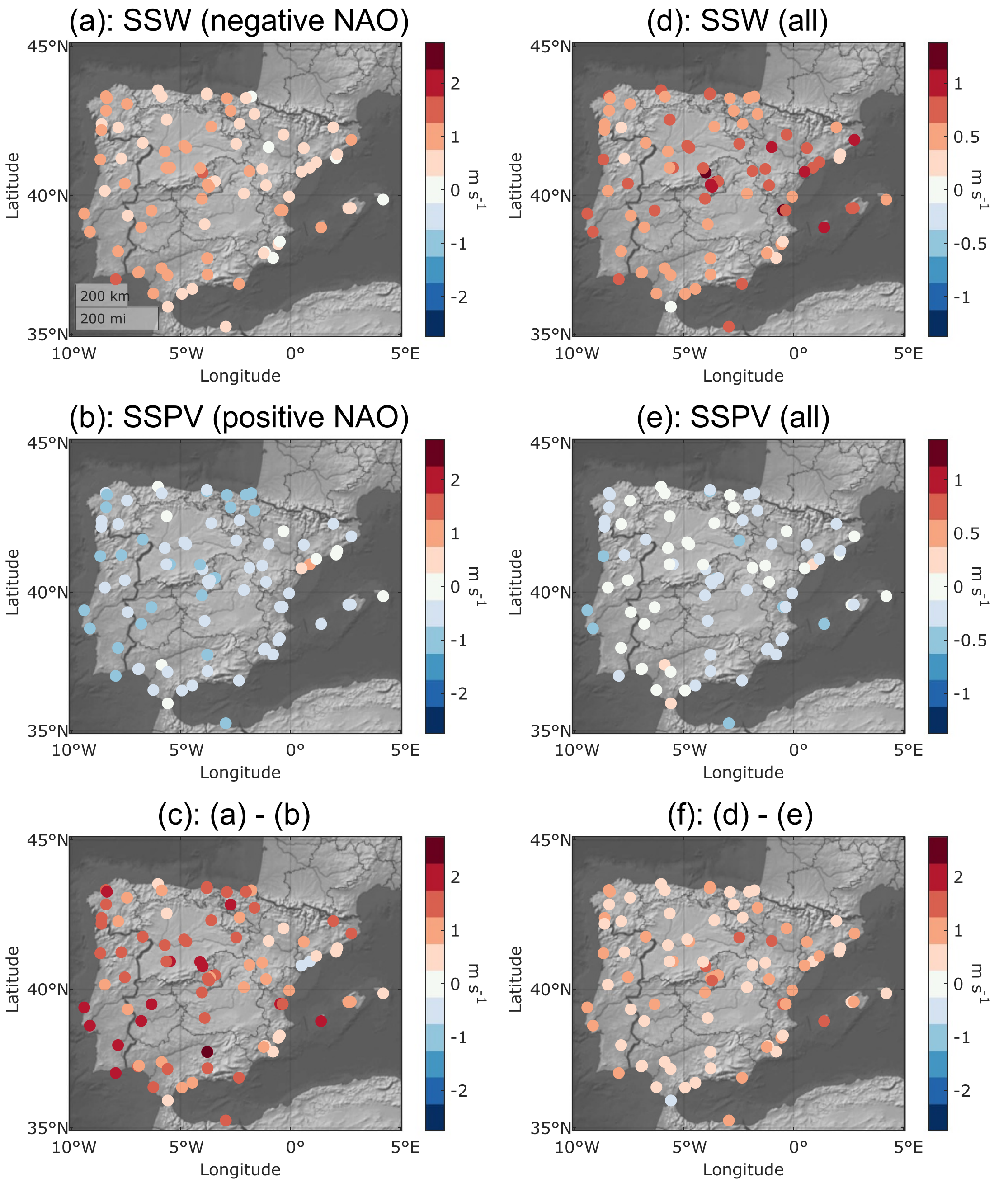

Figure 5. Analysis of observed DPWG anomalies at the 87 stations in the IP following SSW and SSPV events. Panels (a) and (b) depict the 30 d mean DPWG anomalies after SSW and SSPV events, respectively, with tropospheric signals, with panel (c) showing the difference (a)–(b) between these two scenarios. Panels (d) and (e) represent the 30 d mean DPWG anomalies after SSW and SSPV events, respectively, regardless of tropospheric signals, with panel (f) illustrating the difference (d)–(e) between these two scenarios. Different scales have been used in order to appreciate spatial patterns.

approximation to the real signal they may have in the troposphere. In future work, we will follow this signal from the stratosphere to the troposphere, quantifying the travel time, the persistence and the strength of the tropospheric impact. According to Charlton-Perez *et al* (2018), the tropospheric signal following an SSW is of greater magnitude than the SSPV one. However, we did not detect significant differences in either the NAO signal or the DPWG anomalies. It is noteworthy how the DPWG anomaly magnitudes after extreme SPV events are similar when comparing between observations, ERA5, and SPS; being slightly higher in the observations probably due to the smaller sample size.

The SPV can affect the eddy-driven jet location. Generally, an SSW causes a southward shift of the eddy-driven jet (Maycock *et al* 2020), while a strong SPV shifts such jet northward (White *et al* 2020). This agrees with the results found here. However, Afargan-Gerstman and Domeisen (2020) detected one-third of the SSW have no signal in the Atlantic jet which would make the results found here partly diluted.

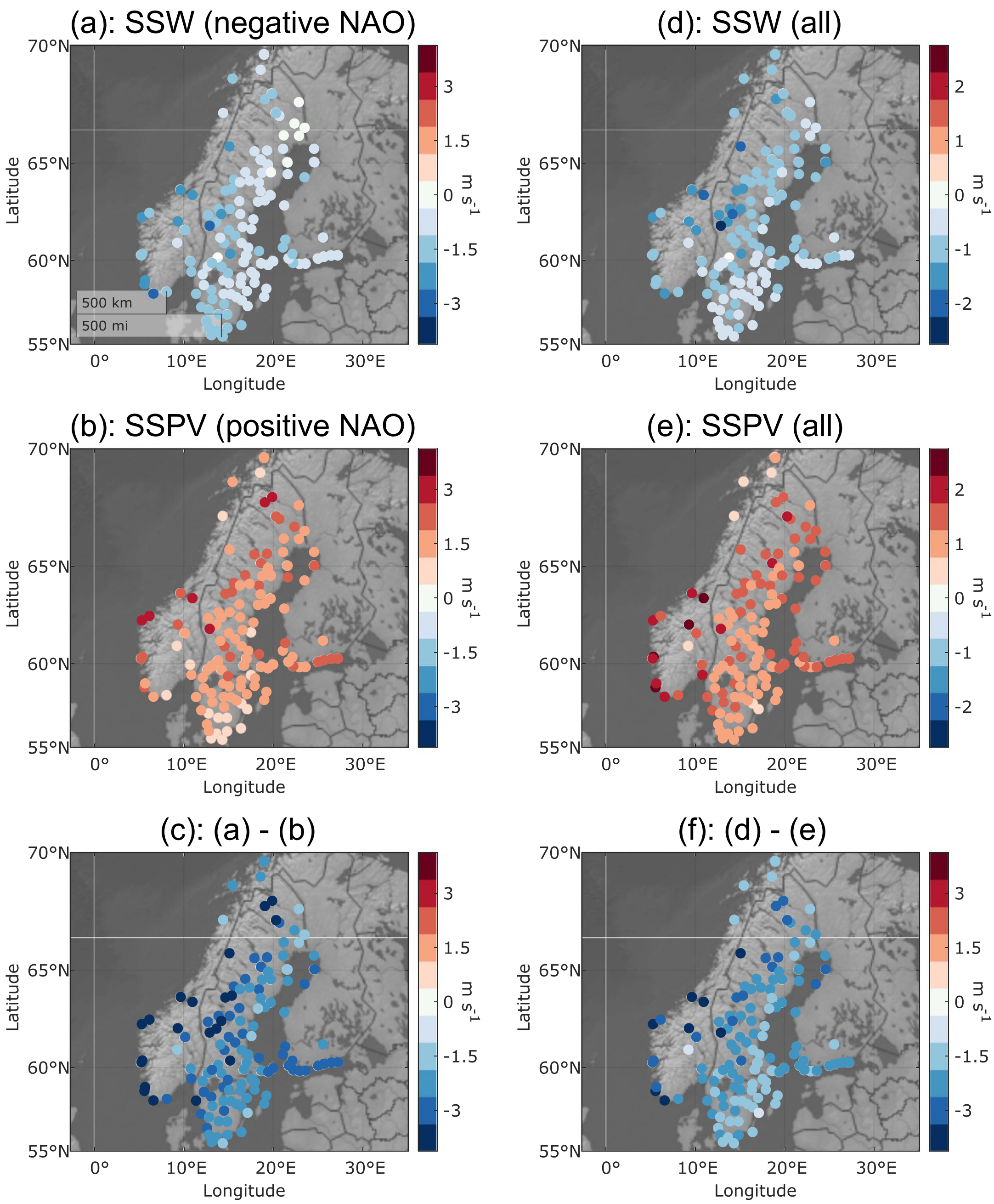

Figure 6. As in figure 5, but for the 127 stations in Scandinavia. Different scales have been used in order to appreciate spatial patterns.

Even some SSW produce a northward shift of the jet depending on the prior tropospheric conditions (Martinez-Andradas *et al* 2023). Therefore, anomalous SPV states are not associated with a unique response in the troposphere, which makes analysis difficult and dilutes the signal (Kolstad *et al* 2022). Averaging over many extreme SPV events removes, to some extent, the effect of the tropospheric preconditions, leaving the net effect regardless of their particularities. Since results here were obtained by averaging over a considerable number of events whose characteristics may vary, part of the signal diversity is lost during the analysis. This becomes more evident when including all extreme SPV events, regardless of whether they have a tropospheric signal or not, where we see how the signal explained above is further diluted. Moreover, not only would the SPV intensity influence the surface, but also its location may play a crucial role (Shen *et al* 2023). Future work should analyse each case individually according to its particularities, for example, how the boreal spring stratospheric final warming would affect DPWG (Hu *et al* 2024).

Similar to near-surface wind speed (Utrabo-Carazo *et al* 2022), extreme SPV events are also not fully correlated with the NAO (Beerli and Grams 2019). Nevertheless, the close relationship between SPV and DPWG shown here could be

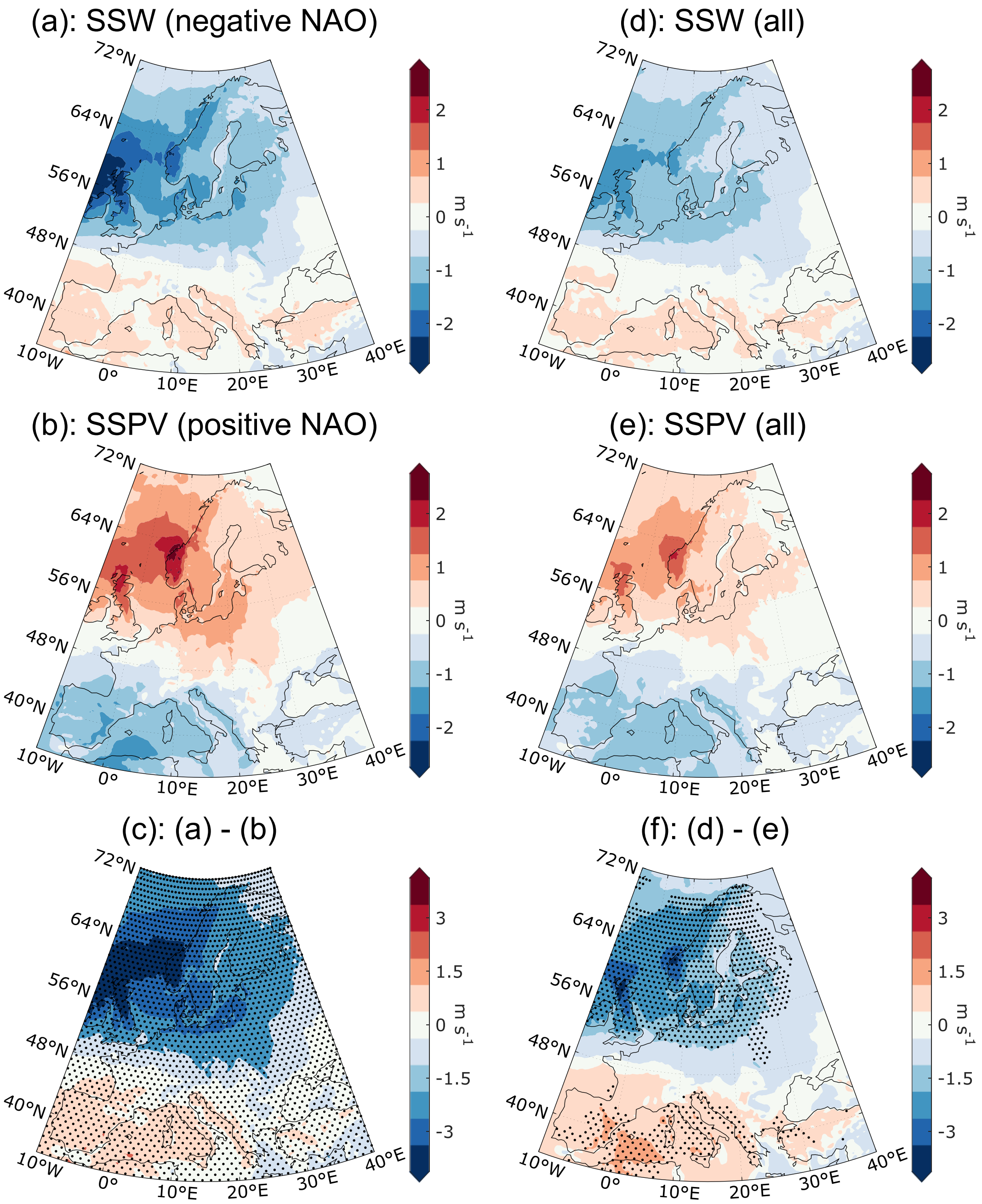

Figure 7. DPWG anomalies from ERA5 renalysis across Europe after SSW and SSPV events. Panels (a) and (b) depict the 30 d mean DPWG anomalies after SSW and SSPV events, respectively, with tropospheric signals, with panel (c) showing the difference (a)–(b) between these two scenarios. Panels (d) and (e) represent the 30 d mean DPWG anomalies after SSW and SSPV events, respectively, regardless of tropospheric signals, with panel (f) illustrating the difference (d)–(e) between these independent scenarios. For (c) and (f), stippling represents significant at $p < 0.01$. Different scales have been used in order to appreciate spatial patterns.

behind the seasonal differences in near-surface wind speed trends between IP and Scandinavia. In the IP, the *stilling* phenomenon is of greater magnitude in winter than for any other season (Utrabo-Carazo *et al* 2022), while for Scandinavia is the opposite (Minola *et al* 2016). Trends in SPV strength could explain the northern *vs.* southern Europe differences in winter near-surface wind speed trends. Büeler *et al* (2020) demonstrated the effects of extreme SPV events depend on the region. Here, DPWG anomalies are greater in absolute value in the North Sea than anywhere else in Europe. Another way to quantify the effects of these extreme events is through the changes in weather patterns they produce (Domeisen *et al* 2020). The DPWG increase after an SSW over the IP could be related to the decrease of anticyclonic weather types and increase of westerlies (not shown here), as they respectively correlate negatively and positively with near-surface wind speed (Utrabo-Carazo *et al* 2022).

Currently, there are uncertainties about why an SSW has a tropospheric signal or not (Bett *et al*

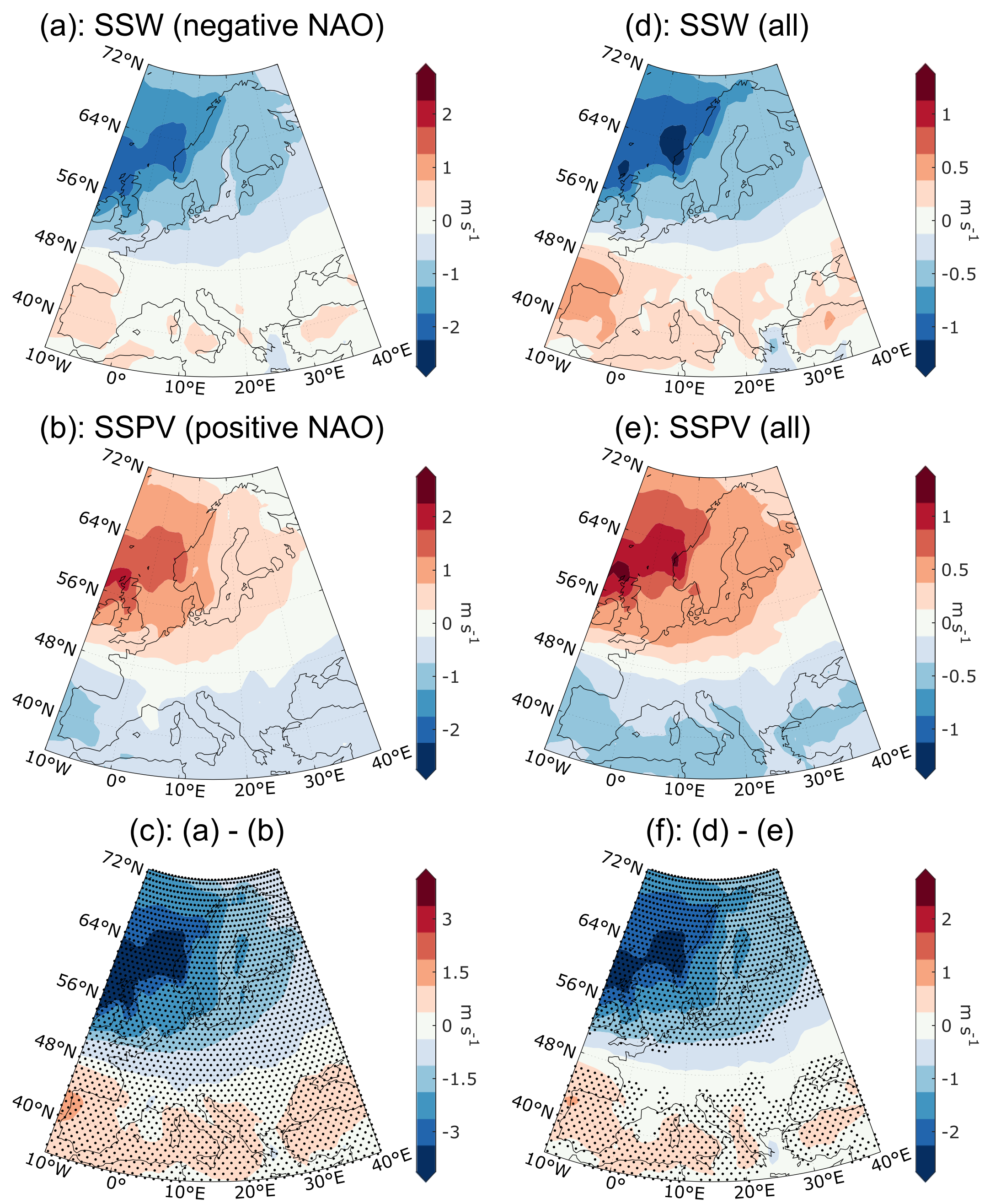

Figure 8. As in figure 7 but for the SEAS5 seasonal prediction system. Different scales have been used in order to appreciate spatial patterns.

2023). White *et al* (2019) determined some precursors that give probabilistic information, but cannot assure if an SSW will have a tropospheric signal or not. Precursors such as ENSO (Oehrlein *et al* 2019) or North Pacific SSTs (Hu *et al* 2021) could influence, but the question is not settled and work remains to be done (Karpechko *et al* 2017). In a climate change scenario, although future projections are uncertain about changes in SSW frequency, models agree the tropospheric effects on the European region will stay the same and the coupling period between the stratosphere and troposphere will extend (Ayarzagüena *et al* 2020). There is also no consensus on SPV changes in magnitude, Domeisen and Butler (2020) discusses two conflicting phenomena affecting the equator-pole air temperature gradient: (a) the Arctic amplification tends to reduce it, and (b) the equatorial upper-troposphere warming tends to increase it. All this makes such studies even more relevant as we expect this predictability source to act for a large part of the year. As shown here, extreme SPV events would be of great help for DPWG forecasts in Europe, which would be useful in many socio-economic fields (e.g. Lledó *et al* 2019).

5. Conclusions

The findings of this research can be summarized as follows:

1. The observed DPWG anomaly distributions are realistically simulated by ERA5, SEAS5 and GloSea6 across the IP and Scandinavia. Since in both regions the DPWG are correlated to the large-scale NAO pattern, we propose that it is highly probable that we can extrapolate the results to the rest of Europe.
2. SEAS5 and GloSea6 partially reproduce the characteristics of the extreme SPV events of ERA5, mainly their tropospheric effects, with the largest differences being in the number of events per winter.
3. The SSW effects on DPWG anomalies are: (a) positive anomalies in southern Europe; (b) negative in northern Europe; and (c) a transition zone of no effect in central Europe. For SSPV events, the impacts are the opposite. The differences between the effects of both types of events are statistically significant for both regions.
4. We find the same effects of extreme SPV events on the spatial patterns and magnitude of DPWG anomalies between observations, ERA5, SEAS5 and GloSea6.
5. The spatial patterns of DPWG anomalies are maintained when comparing between 1–30 and 1–60 d after the events and between considering only those with tropospheric effects and considering all events. Decreasing in magnitude for 1–60 d and when considering all events regardless of whether they have tropospheric effects or not.

Data availability statement

The data that support the findings of this study are openly available at the following URL/DOI: https://doi.org/10.5281/zenodo.11191250. The observed DPWG anomaly series for the IP and Scandinavia can be found at Utrabo-Carazo (2024) (https://github.com/Utrabo-Carazo/ DPWGanom_IP-Scandinavia; last accessed 14 May 2024. ERA5 data were downloaded from ECMWF (https://doi.org/10.24381/cds.adbb2d47; last accessed 14 May 2024). SEAS5 and GloSea6 data were downloaded from the Climate Data Store (https://doi.org/10.24381/cds.181d637e; last accessed 14 May 2024)

Acknowledgments

E U-C was supported by the FPI fellowship (PRE2019-090148). R J H D was supported by the Met Office Hadley Centre Climate Programme funded by DSIT. L M is founded by the International Postdoc grant from the Swedish Research Council (2921-00444). This study was conducted in the framework of the IBER-STILLING Project (RTI2018-095749-A-100; MCIU/ AEI/FEDER,UE); the VENTS Project (GVA-AICO/2021/023); the RED-CLIMA 2 Project (LINCGLOBAL—CSIC, Ref. LINCG24042) and the CSIC Interdisciplinary Thematic Platform (PTI) Clima (PTI—CLIMA). Finally, we acknowledge the rich discussion with the expert groups at the Met Office (UK) during the short research stay conducted in autumn 2023 and funded by the WIND-ATLAS Project (reference 202230I068; CSIC). We acknowledge the two anonymous reviewers for their detailed and helpful comments to the original manuscript.

ORCID iDs

Eduardo Utrabo-Carazo https://orcid.org/0000-0002-9958-2308
Julia F Lockwood https://orcid.org/0000-0003-2596-7341
Robert J H Dunn https://orcid.org/0000-0003-2469-5989
Lorenzo Minola https://orcid.org/0000-0002-3476-1137
Enric Aguilar https://orcid.org/0000-0002-8384-377X
Cesar Azorin-Molina https://orcid.org/0000-0001-5913-7026

References

Afargan-Gerstman H and Domeisen D I V 2020 Pacific modulation of the North Atlantic storm track response to sudden stratospheric warming events *Geophys. Res. Lett.* **47** e2019GL085007

Ayarzagüena B *et al* 2020 Uncertainty in the response of sudden stratospheric warmings and stratosphere-troposphere coupling to quadrupled CO_2 concentrations in CMIP6 models *J. Geophys. Res. Atmos.* **125** e2019JD032345

Ayarzagüena B, Barriopedro D, Garrido-Perez J, Abalos M, de la Cámara A, García-Herrera R, Calvo N and Ordóñez C 2018 Stratospheric connection to the abrupt end of the 2016/2017 Iberian drought *Geophys. Res. Lett.* **45** 12639–46

Baldwin M P *et al* 2021 Sudden stratospheric warmings *Rev. Geophys.* **59** e2020RG000708

Beerli R and Grams C M 2019 Stratospheric modulation of the large-scale circulation in the Atlantic–European region and its implications for surface weather events *Q. J. R. Meteorol. Soc.* **145** 3732–50

Bett P E, Scaife A A, Hardiman S C, Thornton H E, Shen X, Wang L and Pang B 2023 Using large ensembles to quantify the impact of sudden stratospheric warmings and their precursors on the North Atlantic oscillation *Weather Clim. Dyn.* **4** 213–28

Brown L D, Cai T T and DasGupta A 2001 Interval estimation for a binomial proportion *Stat. Sci.* **16** 101–33

Büeler D, Beerli R, Wernli H and Grams C M 2020 Stratospheric influence on ECMWF sub-seasonal forecast skill for energy-industry-relevant surface weather in European countries *Q. J. R. Meteorol. Soc.* **146** 3675–94

Charlton-Perez A J, Ferranti L and Lee R W 2018 The influence of the stratospheric state on North Atlantic weather regimes *Q. J. R. Meteorol. Soc.* **144** 1140–51

Domeisen D and Butler A 2020 Stratospheric drivers of extreme events at the Earth's surface *Commun. Earth Environ.* **1** 59

Domeisen D, Grams C and Papritz L 2020 The role of North Atlantic–European weather regimes in the surface impact of sudden stratospheric warming events *Weather Clim. Dyn.* **1** 373–88
Dunstone N, Smith D, Scaife A, Hermanson L, Eade R, Robinson N, Andrews M and Knight J 2016 Skilful predictions of the winter North Atlantic oscillation one year ahead *Nat. Geosci.* **9** 809–14
Hall R, Mitchell D, Seviour W and Wright C 2021 Tracking the stratosphere-to-surface impact of sudden stratospheric warmings *J. Geophys. Res. Atmos.* **126** e2020JD033881
Hersbach H *et al* 2023 ERA5 hourly data on single levels from 1940 to present *Copernicus Climate Change Service (C3S) Climate Data Store (CDS)* (available at: https://doi.org/10.24381/cds.adbb2d47) (Accessed 8 April 2024)
Hu D, Guan Z, Liu M and Wang T 2021 Is the relationship between stratospheric arctic vortex and arctic oscillation steady? *J. Geophys. Res. Atmos.* **126** e2021JD035759
Hu J, Xie J, Deng J, Yang S and Ren R 2024 The impact of boreal spring stratospheric final warming on surface air temperature over Northern Hemisphere in ERA5 and CMIP6 models *Clim. Dyn.* **62** 3207–19
Johnson S J *et al* 2019 SEAS5: the new ECMWF seasonal forecast system *Geosci. Model Dev.* **12** 1087–117
Karpechko A Y, Hitchcock P, Peters D H W and Schneidereit A 2017 Predictability of downward propagation of major sudden stratospheric warmings *Q. J. R. Meteorol. Soc.* **143** 1459–70
Kay G, Dunstone N J, Maidens A, Scaife A A, Smith D M, Thornton H E, Dawkins L and Belcher S E 2023 Variability in North Sea wind energy and the potential for prolonged winter wind drought *Atmos. Sci. Lett.* **24** e1158
Kidston J, Scaife A A, Hardiman S C, Mitchell D M, Butchart N, Baldwin M P and Gray L J 2015 Stratospheric influence on tropospheric jet streams, storm tracks and surface weather *Nat. Geosci.* **8** 433–40
King A D, Butler A H, Jucker M, Earl N O and Rudeva I 2019 Observed relationships between sudden stratospheric warmings and European climate extremes *J. Geophys. Res. Atmos.* **124** 13943–61
Kolstad E W, Lee S H, Butler A H, Domeisen D I V and Wulff C O 2022 Diverse surface signatures of stratospheric polar vortex anomalies *J. Geophys. Res. Atmos.* **127** e2022JD037422
Lledó L, Torralba V, Soret A, Ramon J and Doblas-Reyes F 2019 Seasonal forecasts of wind power generation *Renew. Energy* **143** 91–100
Lockwood J F, Stringer N, Hodge K R, Bett P E, Knight J, Smith D, Scaife A A, Patterson M, Dunstone N and Thornton H E 2023 Seasonal prediction of UK mean and extreme winds *Q. J. R. Meteorol. Soc.* **149** 3477–89
MacLachlan C *et al* 2015 Global seasonal forecast system version 5 (GloSea5): a high-resolution seasonal forecast system *Q. J. R. Meteorol. Soc.* **141** 1072–84
Martinez-Andradas V, de la Cámara A and Zurita-Gotor P 2023 Stratosphere–troposphere coupling during sudden stratospheric warmings with different North Atlantic jet response *J. Clim.* **36** 6111–24
Maycock A C, Masukwedza G I T, Hitchcock P and Simpson I R 2020 A regime perspective on the North Atlantic eddy-driven jet response to sudden stratospheric warmings *J. Clim.* **33** 3901–17
Minola L *et al* 2023 The contribution of large-scale atmospheric circulation to variations of observed near-surface wind speed across Sweden since 1926 *Clim. Change* **176** 54
Minola L, Azorin-Molina C and Chen D 2016 Homogenization and assessment of observed near-surface wind speed trends across Sweden, 1956–2013 *J. Clim.* **29** 7397–415
Minola L, Azorin-Molina C, Guijarro J A, Zhang G, Son S-W and Chen D 2021 Climatology of near-surface daily peak wind gusts across Scandinavia: observations and model simulations *J. Geophys. Res. Atmos.* **126** e2020JD033534
Minola L, Zhang F, Azorin-Molina C, Pirooz A A S, Flay R G J, Hersbach H and Chen D 2020 Near-surface mean and gust wind speeds in ERA5 across Sweden: towards an improved gust parametrization *Clim. Dyn.* **55** 887–907
Oehrlein J, Chiodo G and Polvani L M 2019 Separating and quantifying the distinct impacts of El Niño and sudden stratospheric warmings on North Atlantic and Eurasian wintertime climate *Atmos. Sci. Lett.* **20** e923
Owen L E, Catto J L, Dunstone N J and Stephenson D B 2021 How well can a seasonal forecast system represent three hourly compound wind and precipitation extremes over Europe? *Environ. Res. Lett.* **16** 074019
Ramon J, Lledó L, Torralba V, Soret A and Doblas-Reyes F J 2019 What global reanalysis best represents near-surface winds? *Q. J. R. Meteorol. Soc.* **145** 3236–51
Scherhag R 1952 Die explosionsartige stratosphärenerwärmung des spätwinters 1951/52 *Ber. Dtsch. Wetterdienstes US-Zone* **6** 51–63
Shen X, Wang L, Scaife A A, Hardiman S C and Xu P 2023 The stratosphere–troposphere oscillation as the dominant intraseasonal coupling mode between the stratosphere and troposphere *J. Clim.* **36** 2259–76
Smith K L, Polvani L M and Tremblay L B 2018 The impact of stratospheric circulation extremes on minimum Arctic sea ice extent *J. Clim.* **31** 7169–83
Tian Q, Huang G, Hu K and Niyogi D 2019 Observed and global climate model based changes in wind power potential over the Northern Hemisphere during 1979–2016 *Energy* **167** 1224–35
Utrabo-Carazo E, Azorin-Molina C, Aguilar E and Brunet M 2023 A spectral analysis of near-surface mean wind speed and gusts over the Iberian Peninsula *Geophys. Res. Lett.* **50** e2023GL103323
Utrabo-Carazo E, Azorin-Molina C, Serrano E, Aguilar E, Brunet M and Guijarro J A 2022 Wind stilling ceased in the Iberian Peninsula since the 2000s *Atmos. Res.* **272** 106153
Waugh D W, Sobel A H and Polvani L M 2017 What is the polar vortex and how does it influence weather? *Bull. Am. Meteorol. Soc.* **98** 37–44
White I P, Garfinkel C I, Gerber E P, Jucker M, Hitchcock P and Rao J 2020 The generic nature of the tropospheric response to sudden stratospheric warmings *J. Clim.* **33** 5589–610
White I, Garfinkel C I, Gerber E P, Jucker M, Aquila V and Oman L D 2019 The downward influence of sudden stratospheric warmings: association with tropospheric precursors *J. Clim.* **32** 85–108
Wilson E B 1927 Probable inference, the law of succession and statistical inference *J. Am. Stat. Assoc.* **22** 209–12
Zhou L, Liu H, Jiang X, Ziegler A D, Azorin-Molina C, Liu J and Zeng Z 2022 An artificial intelligence reconstruction of global gridded surface winds *Sci. Bull.* **67** 2060–3